Image Cover Sheet

CLASSIFICATION	SYSTEM NUMBER 518147
UNCLASSIFIED	

TITLE

Effects of Bridge Pattern on Performance of YBaCuO Microbolometers

System Number:

Patron Number:

Requester:

Notes:

DSIS Use only:

Deliver to: CL

THIS PAGE IS LEFT BLANK

THIS PAGE IS LEFT BLANK

Reprinted from

Journal of Vacuum Science & Technology A

JVST A

Second Series
Volume 20, Number 5
September/October 2002

Effects of bridge pattern on performance of YBaCuO microbolometers

P. Laou and L. Ngo Phong
Defence Research Establishment Valcartier, 2459 Pie-XI Boulevard, N., Val-Belair, QC G3J 1X5, Canada

pp. 1802-1807

An official journal of the American Vacuum Society
Published for the Society by the American Institute of Physics

Effects of bridge pattern on performance of YBaCuO microbolometers

P. Laou[a)] and L. Ngo Phong
Defence Research Establishment Valcartier, 2459 Pie-XI Boulevard, N., Val-Belair, QC G3J 1X5, Canada

(Received 18 January 2002; accepted 3 June 2002)

The effects of bridge pattern on the performance of YBaCuO microbolometers were investigated. For this purpose, Si_3N_4 bridges with grids and hinges of varying width were created on Si wafers by means of bulk Si micromachining. Semiconducting YBaCuO films were sputter-deposited onto the bridges to form resistive bolometers. In reducing the width of the hinges from 10 to 5 μm, one can enhance the bolometric responsivity by approximately two times at room temperature. Further, a factor of enhancement of as large as three could be achieved on bridges with a grid pattern. The grid pattern also modified the spectral absorbance of the bridges. The enhancement of experimental responsivity was shown to be consistent with the one predicted from changes in thermal conductance, electrical resistance, and optical absorbance of the bolometers. © *2002 American Vacuum Society.* [DOI: 10.1116/1.1496784]

I. INTRODUCTION

Recent years have seen the widespread use of room-temperature microbolometers as sensor elements of thermal infrared imagers.[1,2] Although these imagers are free of the drawbacks inherent to cryogenic systems, their detection range is limited by the relatively low sensitivity of bolometers. For their performance to approach that of traditionally cryogenic imagers, the ultimate bolometric sensitivity must be achieved at room temperature. One approach toward this end is to reduce the heat transfer rate from the bolometer to its surrounding.[3] We fabricated lately resistive YBaCuO microbolometers on thermally isolated Si_3N_4 bridges on Si wafer.[4] As the heat transfer rate is governed in part by the bridge pattern, the effect of the latter on the sensitivity of YBaCuO microbolometers has been studied. The results of this study are reported in this article.

The bolometric responsivity r of a resistive bolometer with a temperature coefficient of resistance β is expressed as

$$r=\frac{I_b R \beta \eta}{G(1+\omega^2\tau^2)^{1/2}}, \qquad (1)$$

where η, R, and τ are, respectively, the optical absorbance, electrical resistance, and time constant of the bolometer, I_b is the bias current to the bolometer, G is the thermal conductance between the bolometer and its surrounding, and ω is the modulation frequency of incident radiation. β is defined as $(1/R)(dR/dT)$ where T is the temperature. All these device parameters have a direct effect on r. Referring to this relation, it is imperative that the bolometer be created on bridges with a pattern such that R is large and G is small. In this work, we first investigated the effect of reducing the width of the hinge of the bridge on the reduction in G. Second, we examined the effect of creating a grid pattern on the bridge. Such a pattern lengthened the electrical path of the bolometer and, therefore, would increase R in the latter. Although the active area of the grid bolometer is equally reduced, a portion of the incident radiation is reflected by the Si back wafer and may be recaptured by the bolometer. Because the grid pattern may also alter the spectral response of the bolometer, this effect was further investigated. In the following sections, we report on the details of the bridge patterns, the processes used to fabricate the bolometers with these bridges, and the effects of the grid patterns on the performance of the fabricated bolometers.

II. DEVICE FABRICATION

The wafers used in this work were made of n-type (100) Si. These wafers were coated with a 600 nm thick Si_3N_4 layer using plasma enhanced chemical vapor deposition. A thin, sacrificial Cr layer was sputter-deposited onto the Si_3N_4 by magnetron rf sputtering. This layer serves as a mask for the transfer of the bridge pattern onto the Si_3N_4 layer. After the etching of selected areas of the Si_3N_4 layer, the Cr layer was removed. This was followed by the bulk Si micromachining using an anisotropic Si etchant (KOH solution). Once the wafer areas under the Si_3N_4 bridge areas were removed, suspended Si_3N_4 bridges where the active regions located were formed on the wafer. After this, YBaCuO and Au films were sputter-deposited successively onto the bridges without breaking the vacuum of the deposition chamber. The thicknesses of the YBaCuO and Au films were, respectively, 100 and 50 nm. The resistivity of the YBaCuO film was about 10 Ω cm. The YBaCuO and Au films were subsequently patterned by standard photolithography to complete the fabrication. The bolometers were mounted onto standard microelectronic packages for the characterization experiments. Thermosonic wire bonding was performed to attach Au leads with a diameter of 17 μm to the Au contact pads on the bolometers.

Figure 1 shows the bridges of the bolometers investigated in this work. They include: (i) bridges with 10 μm wide and 70 μm long hinges (bridge A), (ii) bridges with 5 μm wide and 75 μm long hinges (bridge B), (iii) bridge A with a grid formed by two 10×40 μm^2 windows on the bridge area (bridge C), and (iv) bridge A with a grid formed by six 3.5×40 μm^2 windows on the bridge area (bridge D). Unless

a)Electronic mail: philips.laou@drdc-rddc.gc.ca

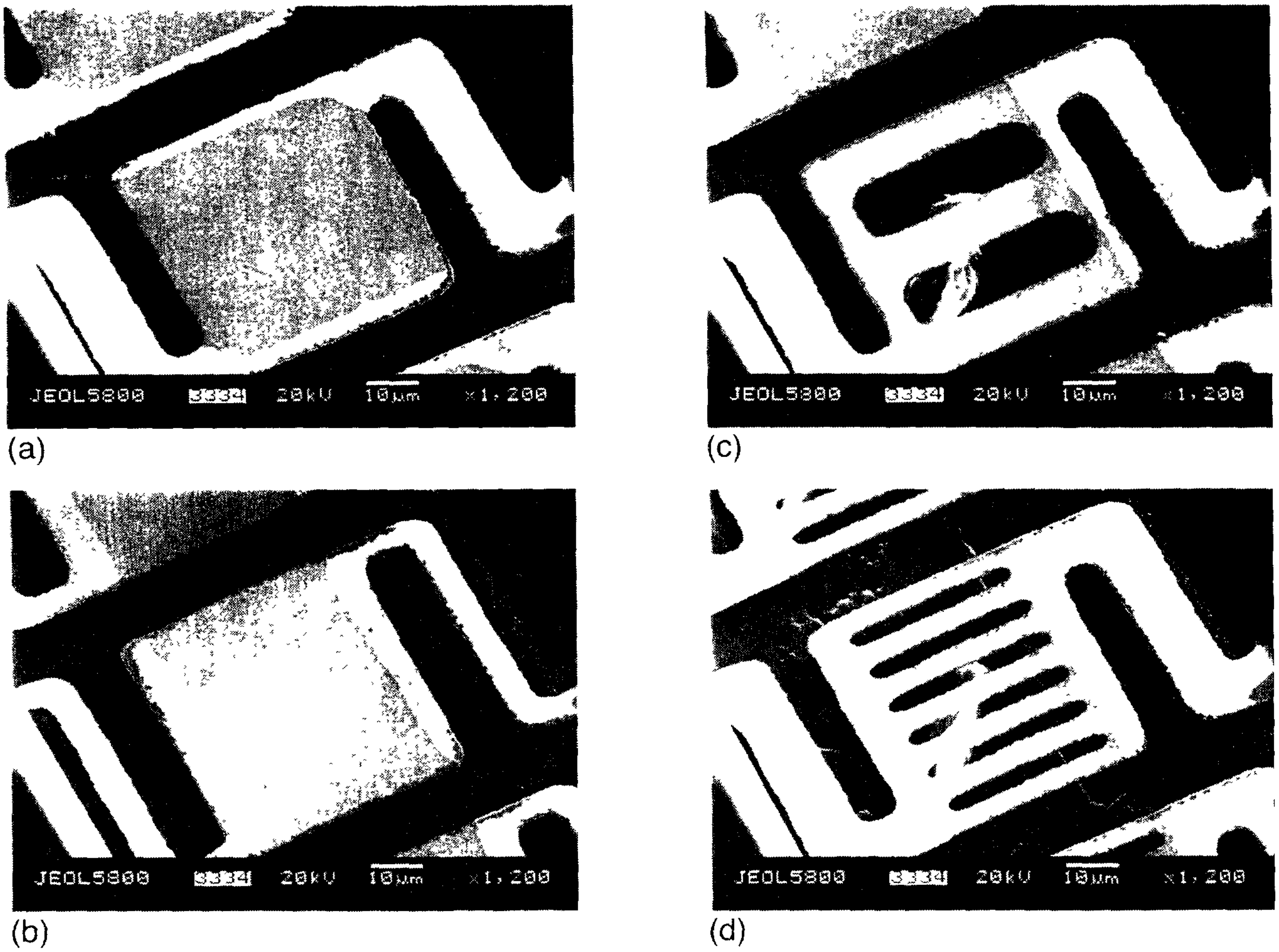

FIG. 1. Scanning electron microscopy photographs of microbolometers with (a) 10 μm wide hinges (bridge A) (b) 5 μm wide hinges (bridge B), (c) 10 μm wide hinges and two 10 μm wide windows (bridge C), and (d) 10 μm wide hinges and six 3.5 μm wide windows (bridge D).

stated otherwise, for all four bridges the active area was $50\times50\ \mu m^2$. Hereafter, the device parameters of the bolometers having different bridge patterns will be denoted with the bridge letter identified in subscript (e.g., R_A is the electrical resistance of bolometer having bridge A; η_B is the optical absorbance of bolometer having bridge B, etc.) To facilitate the comparison, bolometers with different bridges were fabricated on the same wafer, i.e., the film properties of Au, YBaCuO, and Si_3N_4 remained unchanged among all the bolometers.

III. EXPERIMENTAL PROCEDURES

The purpose of the experiments is to determine the bridge configuration with the highest sensitivity, among those investigated for the bolometer. Toward this end, responsivities of different bolometers were measured and compared. Further, for a better understanding of the effect of the bridge parameters on the bolometric responsivity, the parameters associated with each bridge configuration are extracted separately. The parameters examined in this work are R, β, G, τ, and η.

In the first series of experiments, the bolometric responsivity was measured at room temperature for each configuration. The incident radiation was obtained from a glow bar and was modulated mechanically with a chopper. The root-mean-square (rms) power density of radiation incident onto the bolometer was $\sim1.4\times10^{-4}$ W/cm^2. A low noise current source provided constant currents in the bolometer, I_b, of up to several tens of μA. The rms voltage fluctuation under a dark condition (noise, V_n) or in the presence of radiation (photoresponse, V) was detected by a lock-in amplifier.

The electrical resistance R of YBaCuO bolometers was measured as a function of the temperature in the range of 280 to 320 K and in a vacuum pressure of ~1 mTorr. Control to within 10 mK in this temperature range was achieved by means of a thermometer, temperature controller, and heater in a feedback loop. The resistance of the bolometer was obtained by measuring the voltage developed across the electrodes with a nanovoltmeter. From the slope of the $R-T$ characteristic, the coefficient β of the bolometer could be derived. In this experiment, a small bias current ($\sim0.1\ \mu$A) was specifically used in order to minimize the Joule heating of the device. The thermal conductance G was derived in a vacuum pressure of ~1 mTorr by estimating the amount of resistive heat needed to raise the bolometer temperature by

TABLE I. Parameters associated with different bridge patterns of bolometers

Bridge	A	B	C	D
Area (10^{-5} cm^2)[a]	2.5	2.5	1.7	1.8
R (10^6 Ω)[b]	0.92	0.83	1.40	1.72
β (%/K)	2.30	2.30	2.20	2.36
G (10^{-6} W/K)	2.59	1.87	2.76	2.39
τ (10^{-3} s)	0.99	1.48	0.70	0.79
η	0.31	0.44	0.49	0.50
r_{comp} (V/W)[c]	12 663	22 458	27 379	42 460
$r_{measured}$ (V/W)[b]	11 264	21 524	24 912	38 628

[a]The active areas of bridges C to D are estimated from scanning electron microscopy photographs.
[b]The bias currents of bridges A to D are 5.0 μA
[c]r_{comp} of bridges A to D are computed directly from the bolometer parameters R, β, G, η and I_b with I_b equal to 5.0 μA.

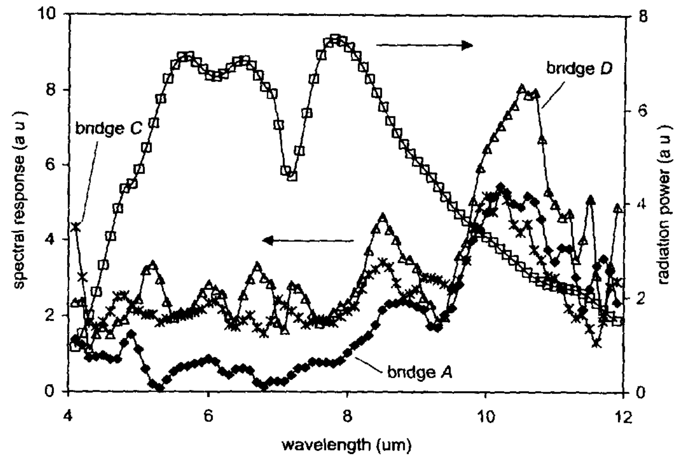

FIG. 2. Spectral response of the bolometers having different bridges

one degree from room temperature. The resistive heating of the bolometer was performed by supplying a constant current to it, in the absence of radiation heating. By making use of the R–T characteristic of the bolometer, the temperature increase in the latter was determined by measuring the decrease in resistance. The time constant of the bolometer was determined from the measurement of responsivity as a function of the frequency. By fitting the latter with the theoretical bolometric responsivity $r = r_0(1+4\pi^2 f^2 \tau^2)^{-1/2}$, one can obtain the numerical solutions of r_0 and τ, where $r_0 = I_b R \eta\beta/G$. With the knowledge of r_0, one can estimate η. After all the parameters were determined, it is possible to compute the responsivity, r_{comp}, from Eq. (1) so as to access the accuracy of experimental responsivity $r_{measured}$.

In the second series of experiments, the bolometric responsivities of different bolometers were measured as a function of the radiation wavelength. The spectral measurement was performed in the range of 1 to 13 μm by using a precision monochromator. The purpose of these experiments was to determine the effect of the bridge configuration on the spectral dependence of responsivity. These results also provided insight into the overall effect of the bridge configurations.

IV. RESULTS AND DISCUSSION

The effects of bridge patterns on r were investigated. The investigation was performed on up to six microbolometers per bridge pattern. Table I summarizes the different parameters of the bolometers associated with these bridges at room temperature. The experimental parameters were extracted directly or indirectly using the methods described in Sec. III.

Assuming that all bolometers have identical film thickness and resistivity, R is proportional to the aspect ratio (length/width) of the active YBaCuO area of the bridge. Referring to Fig. 1, the aspect ratio of bridge A is 1/0.85 times that of bridge B. Table I shows, accordingly, that R_A is 1/0.9 times R_B. With respect to bridges A and B, bridges C and D show larger values of R because of their smaller width of the electrical path of their patterns. In fact, these bridges contain, respectively, three and seven resistors (see Fig. 1) connected in parallel. On the basis of pattern geometry, R_D should be larger than R_A by a factor of 1.7 and 1.8, respectively. This estimation is consistent with the measured R_C and R_D shown in Table I. The temperature coefficients of resistance β of the bridge are almost identical, regardless of the bridge patterns. This result is anticipated as the properties of the YBaCuO films deposited on the bridges should be identical.

The thermal conductance of the bolometer is defined mainly by the thermal link between the suspended bridge and the Si substrate. Since this thermal link consists of the hinges of the bridge, the conductance G of the bolometer is expected to be proportional to the width of the hinges. From the measured values of G, it is seen that the bolometer having the narrowest hinges, exhibits the smallest G (bridge B). Besides R, β, and G, τ, and η are two remaining parameters which vary with the bridge patterns. The data in Table I shows that, τ_B is 50% larger than τ_A. This may be due to the fact that the heat dissipation rate in bridge B is smaller than that of bridge A. The experimental result also shows that τ_C and τ_D are 70% and 80% of τ_A, respectively. The reductions of τ_C and τ_D may be explained by comparing their heat capacitances where $C \sim \tau G$ when G is kept unchanged. The heat capacitance of the Si_3N_4 bridge could be derived from the volume of the structure, density, and specific heat of Si_3N_4. For bridges A and B, the volume is 1.5×10^{-9} cm^3. Using a density of 3.44 g/cm^3 and a specific heat of 0.17 J/g K for Si_3N_4, the heat capacitance of the bridge is estimated to be 8.8×10^{-10} J/K. For bridge C (1.00×10^{-9} cm^3 in volume) and D (1.02×10^{-9} cm^3 in volume), the heat capacitances are 5.8×10^{-10} J/K, and 6.0×10^{-10} J/K, respectively. The ratio of τ between bridge patterns appears to be consistent with the ratio between the heat capacitances.

The optical absorbance η associated with each bridge pattern is shown in Table I. It is seen that η_B, η_C, and η_D are, respectively, 42%, 58%, and 61% larger than η_A. This result indicates that bridges B, C, and D are more efficient than bridge A in capturing the incident radiation. It should be noted that the optical absorbance is wavelength dependent and the estimated values of η are average values to broadband radiation. Since the power density of the glow bar is a function of the wavelength, the increased r that was reflected

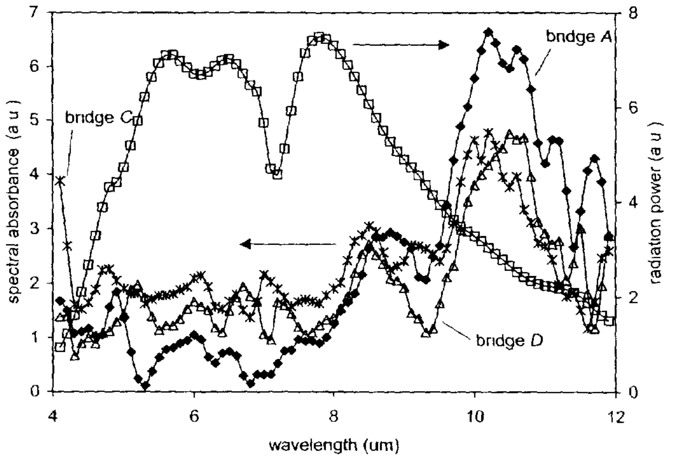

FIG. 3 Spectral absorbance of the bolometer having different bridges

from the increased η may be caused by an overall increase in the spectral absorbance or by large absorbance only at certain wavelengths. Since R, β, and G are not spectrally dependent, it is possible to remove the contributions of R, β, and G from the results of spectral response measurements according to Eq. (1). As a result, one can obtain the optical absorbances of the bolometers having different bridges as a function of the wavelength, η_s.

Figure 2 shows the relative spectral response measured on the bolometers having bridges A, C, and D. The power density of the glow bar as a function of the wavelength was also illustrated in Fig. 2 for reference. It is seen that the bolometers which have bridges with grids have larger responses. This is due to the fact that the presence of grids helps increase R and η. The same result was obtained from the broadband measurement as shown in Table I. The contribution of R, β, and G to the spectral response were then removed from each curve in Fig. 2 according to Eq. (1). The relative η_s was illustrated in Fig. 3. It is clear that the profiles of the η_s of bridges C and D matched closely and this is reflected from the estimated η_C and η_D in Table I. r_D is larger than r_C because of a larger R_D. Also, it can be seen in Fig. 3 that bridge A exhibits small absorbance in the region at short wavelengths and large absorbance at long wavelengths. Because the power density of the glow bar peaks near short wavelengths, r_A is smaller than r_C and r_D. This result confirms the fact that the increased optical absorbance is attributed to large absorbance at certain wavelengths.

With the knowledge of R, β, G, η, and I_b, it is possible to compute r_{comp} by using Eq. (1). Referring to Table I, the computed responsivities of bridges A to D are generally in good agreement with the experimental ones. This confirms that the characteristics of the different bridge patterns could be accurately derived from a conventional bolometric model. Using bridge A as a reference, the responsivity of the bridge is enhanced by about two times and that of bridges C and D by three times. The magnitudes of enhancement is consistent with the modifications of bolometer parameters, in the case of bridge B, a decrease in G and an increase in η, and in the cases of bridges C and D, an increase in both R and η.

V. CONCLUSIONS

The effects of bridge patterns on the performance of YBaCuO microbolometers were investigated. The results show that bridges with a smaller hinge width have smaller thermal conductance, which improves the bolometric responsivity. In reducing the width of the hinges from 10 to 5 μm, the bolometric responsivity was enhanced by approximately two times at room temperature. The use of bridges with grids also resulted in enhanced responsivity. This enhancement is attributed to the increases in electrical resistance and optical absorbance of the bolometer. The measured responsivity was shown to be consistent with the one estimated from the extracted parameters. By removing the contributions of resistance and thermal conductance to the spectral response of bridges A, C, and D, it was shown that the bridges with grids have modified optical absorbance which have a spectral profile of large absorbance in the region of short wavelengths and small absorbance in the region of long wavelengths, not an overall increase in optical absorbance. This modification is useful to applications in which the region of interest is in the short wavelengths.

[1]H. Nef *et al.*, Appl. Phys. Lett. **66**, 2421 (1995).
[2]S. J. Berkowitz, A. S. Hirahara, K. Char, and E. N. Grossman, Appl. Phys. Lett. **69**, 2125 (1996).
[3]K. C. Liddiard, November 29, 1994. U.S. Patent No. 5 369 280.
[4]L. N. Phong and S. N. Qiu, J. Vac. Sci. Technol. A **18**, 635 (2000).

518147